DOI: 10.1002/asia.201100176

Synthesis and Photophysical Properties of Dimethoxybis(3,3,3-trifluoropropen-1-yl)benzenes: Compact Chromophores Exhibiting Violet Fluorescence in the Solid State

Masaki Shimizu,* Youhei Takeda, Masahiro Higashi, and Tamejiro Hiyama[a]

Abstract: Dimethoxybis(3,3,3-trifluoropropen-1-yl)benzenes were prepared through palladium-catalyzed double cross-coupling reactions of diiododimethoxybenzenes with $CF_3C{\equiv}CZnCl$, followed by reduction of $CF_3C{\equiv}C$ groups with $LiAlH_4$ or H_2 in the presence of the Lindlar catalyst. The edges of the absorption spectra of 1,2-$(MeO)_2$-4,5-$(CF_3CHC{=}CH)_2$benzenes **1** and 1,3-$(MeO)_2$-4,6-$(CF_3CH{=}CH)_2$benzenes **2** in cyclohexane ranged from 348 to 360 nm, whereas the absorption spectra of 1,4-$(MeO)_2$-2,5-[(*E*)-$CF_3CH{=}CH]_2$ benzene ((*E*)-**3**) ended at 406 nm. These findings indicate that the effective conjugation length of (*E*)-**3** was significantly larger than those of **1** and **2**. Consistently, **1** and **2** in cyclohexane exhibited fluorescence with emission maxima in the UV region, whereas (*E*)-**3** in cyclohexane emitted violet light with an emission maximum at 407 nm. All the fluorescence spectra of **1**–**3** in various solvents redshifted as the solvent polarity increased. The photoluminescence of **1**–**3** in the solid states was also observed with emission maxima in the violet region. It is important to note that the quantum yields of (*E*)-**3** in a neat thin film and in a doped polymer film were 0.37 and 0.49, respectively. Density functional theory calculations suggested that the fluorine atoms contribute to a slight extension of both the HOMOs and the LUMOs, as well as narrowing of the HOMO–LUMO gaps when compared with the corresponding fluorine-free analogues. In the case of (*E*)-**3**, it is suggested that the HOMO–LUMO transition includes charge transfer from the ethereal oxygen atoms to the $C(sp^2){-}CF_3$ moieties.

Keywords: chromophores · fluorescence · fluorine · materials science · molecular electronics

Introduction

Fluorinated π-conjugated molecules have attracted considerable attention in the field of functional organic materials because the presence of fluorine atoms in organic molecules endows the molecules with unique chemical and physical properties, which are distinct from those of their nonfluorinated counterparts.[1] Originated from the highest electronegativity of fluorine among all elements, fluorinated alkyl and ethenyl groups and per- and semifluorinated aromatic rings induce various attractive characteristics, such as excellent thermal and oxidative stabilities, high electron affinity, and weak intermolecular interactions, that are effective for precise control of molecular assembly. Typical examples of fluorine-containing electron-transporting semiconductor materials include perfluoropentacene,[2] perfluorinated oligo(*p*-phenylene)s,[3] perfluoroalkylated oligothiophenes,[4] 4-perfluoroalkylphenyl-substituted oligoarylenes,[5] and perfluoroalkylene-bridge-containing oligothiophenes.[6] Fluorinated oligo- and poly(phenylenevinylene)s are designed to enhance the electron mobility and tune the emission color of their nonfluorinated counterparts.[7] A wide variety of liquid crystalline compounds that possess fluorine atoms in a mesogenic core, linking groups, and/or terminal chains, have been designed and characterized; thus, systematic studies on the influence of fluorine substituents on the properties of these compounds have led to the development of superior liquid crystals.[8] Therefore, exploration and characterization

[a] Prof. Dr. M. Shimizu, Dr. Y. Takeda, M. Higashi, Prof. Dr. T. Hiyama[+]
Department of Material Chemistry
Graduate School of Engineering, Kyoto University
Kyoto University Katsura, Nishikyo-ku
Kyoto 615-8510 (Japan)
Fax: (+81) 75-383-2445
E-mail: m.shimizu@hs2.ecs.kyoto-u.ac.jp

[+] Current address:
Research & Development Initiative
Chuo University
1-13-27 Kasuga, Bunkyo-ku
Tokyo 112-8551 (Japan)

Supporting information for this article is available on the WWW under http://dx.doi.org/10.1002/asia.201100176.

of novel fluorinated π-conjugated compounds that exhibit unique properties owing to fluorine, are of particular interest in view of the advancement of functional organic materials.

Considerable attention has been given to π-conjugated compounds that emit visible light in the solid state because they have the potential for use in optoelectronic devices, such as organic light-emitting diodes (OLED),[9] organic light-emitting field-effect transistors,[10] semiconductor lasers,[11] and fluorescent sensors.[12] However, it is difficult to develop organic chromophores exhibiting efficient solid-state emission because the molecular aggregation of chromophores in the solid state generally results in severe concentration quenching of luminescence. Accordingly, examples of organic solids that exhibit intense emission in the visible region with high efficiency are extremely limited.[13]

The common structural feature of intensely emissive organic solids that have been developed to date is that they contain multiple aromatic rings and/or polycyclic aromatic hydrocarbon skeletons. The presence of multiple aromatic rings in a molecule often causes a solubility problem, which is one of the undesirable factors that hampers purification and processing of organic materials. Hence, it is of great interest to develop organic chromophores that exhibit high luminescence efficiency in the solid state with a minimum number of benzene rings as the aromatic component. To this end, we recently showed that 1,4-bis(alkenyl)-2,5-dipiperidinobenzenes exhibit highly efficient solid-state fluorescence in the spectral region ranging from blue to red, which can be tuned by selection of appropriate alkenyl groups.[14] The molecular design of diaminobis(alkenyl)benzenes originated from our serendipitous finding that 1,2-dimethoxy-4,5-bis[(*E*)-3,3,3-trifluoropropenyl]benzene ((*E*)-**1**), which was obtained as an unexpected product in the attempted Bergman cyclization of 1,2-dimethoxy-4,5-bis(3,3,3-trifluoropropynyl)benzene, was faintly violet-emissive on a TLC plate upon irradiation with a UV lamp at 365 nm. This observation prompted us to examine the properties of benzene derivatives characterized by the substitution of two dimethoxy groups and two 3,3,3-trifluoropropenyl moieties as novel and compact chromophores that emitted visible light in the solid state. Reported herein are the preparation, structures, photophysical properties, and theoretical calculations of dimethoxybis(3,3,3-trifluoropropenyl)benzenes **1**–**3**.

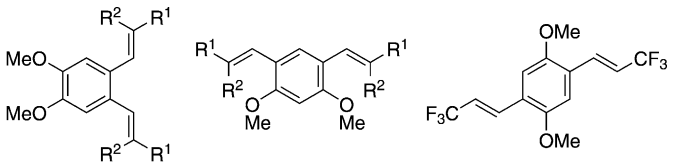

(*E*)-**1** (R^1 = CF_3, R^2 = H) (*E*)-**2** (R^1 = CF_3, R^2 = H) (*E*)-**3**
(*Z*)-**1** (R^1 = H, R^2 = CF_3) (*Z*)-**2** (R^1 = H, R^2 = CF_3)

Results and Discussion

Preparation of Dimethoxybis(3,3,3-trifluoropropenyl)benzenes

Dimethoxybis(3,3,3-trifluoropropenyl)benzenes **1**–**3** were prepared by reduction of the corresponding bis(3,3,3-trifluoropropynyl)benzenes, which were prepared by a double cross-coupling reaction of diiododimethoxybenzenes with in situ generated 3,3,3-trifluoropropynylzinc chloride (**5**).[15] Thus, treatment of 1,1-dichloro-3,3,3-trifluoro-2-tosyloxypropene (**4**) with two equivalents of BuLi in tetrahydrofuran at −78 °C followed by the addition of $ZnCl_2$•TMEDA generated **5**, which was coupled with 4,5-diiodo-1,2-dimethoxybenzene (**6**) in the presence of [$PdCl_2$(dppf)] (dppf = 1,1′-bis(diphenylphosphino)ferrocene; 10 mol%) and Ag_2O (1 equiv) to give bis(3,3,3-trifluoropropynyl)benzene **7** in 72% yield (Scheme 1).[16] Stereoselective reduction of **7** with $LiAlH_4$ gave (*E*)-**1**, whereas (*Z*)-**1** was prepared in high yield by hydrogenation of **7** with the aid of the Lindlar catalyst.

Two-fold cross-coupling reaction of 1,3-diiodobenzene **8** with **5** was catalyzed by 10 mol% of [$Pd(PPh_3)_4$] to give **9** in 69% yield (Scheme 2).[17] Both (*E*)-**2** and (*Z*)-**2** were prepared from **9** in a manner similar to that used to prepare **1**.

When $LiAlH_4$ reduction of 1,4-diethynylbenzene **11** prepared from 1,4-diiodobenzene **10** with **5** was attempted, the reaction resulted in the production of a complex mixture.

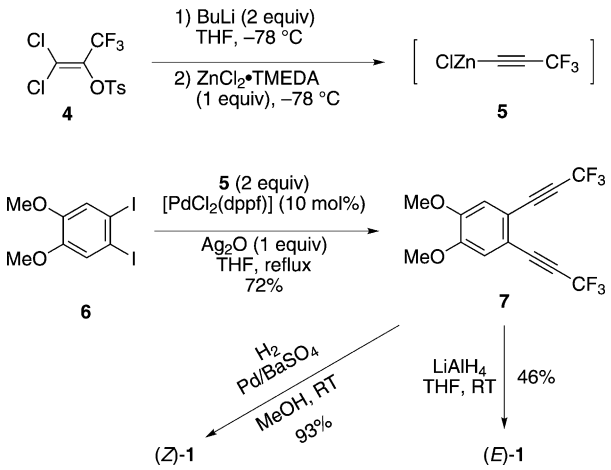

Scheme 1. Synthesis of **1**. THF = tetrahydrofuran.

Abstract in Japanese:

パラジウム触媒を用いてジヨードジメトキシベンゼンとトリフルオロプロピニル亜鉛反応剤との二重交差カップリングを行い、得たビス（トリフルオロプロピニル）ベンゼンを水素化アルミニウムリチウムで還元もしくはLindlar 還元することにより、ジメトキシビス（トリフルオロプロペニル）ベンゼン誘導体を五種類合成した。シクロヘキサン中では、1,4-ジメトキシ-2,5-ビス（トリフルオロプロペニル）ベンゼンのみが紫色の可視光発光を示し、他の誘導体は紫外領域で蛍光を示した。それに対し、固体状態では合成した誘導体はいずれも紫色の蛍光を発した。特に、1,4-ジメトキシ-2,5-ビス（トリフルオロプロペニル）ベンゼンの蛍光量子収率は、薄膜状態で 0.37、ポリ（メチルメタクリレート）フィルムに分散した状態で 0.49 を記録した。理論計算により、この短い共役系からの可視光発光は、メトキシ基からトリフルオロプロペニル基への分子内電荷移動により生じる一重項励起状態からの発光と考えられる。

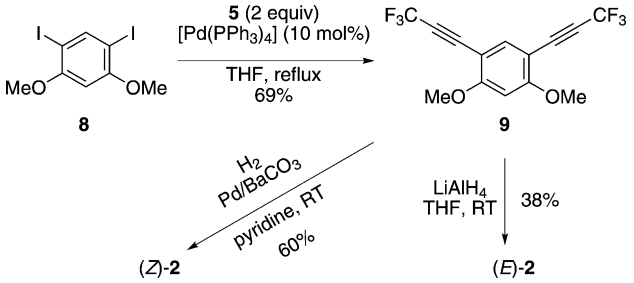

Scheme 2. Synthesis of **2**.

Conversely, hydrogenation of **11** with the Lindlar catalyst gave the expected (*Z*)-**3** quantitatively, the *Z* configuration of which was confirmed based on the coupling constant between the two olefinic hydrogen atoms ($J = 12.4$ Hz) in the crude products (Scheme 3). However, purification of the crude products by column chromatography on silica gel easily caused *Z*–*E* isomerization of (*Z*)-**3** to give a 2:1 mixture of (*Z*)-**3** and (*E*)-**3**. Irradiation of the *Z*/*E* mixture by using a UV lamp in the presence of a catalytic amount of iodine induced complete isomerization of (*Z*)-**3** to (*E*)-**3**; therefore, (*E*)-**3** was isolated as a sole product in good yield.

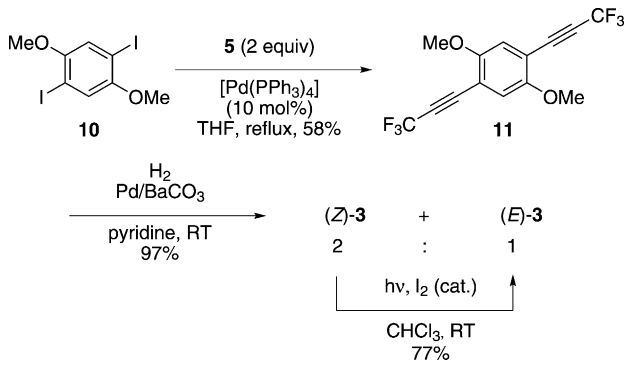

Scheme 3. Synthesis of (*E*)-**3**.

Photophysical Properties

The UV/visible absorption spectra of **1**–**3** were measured in various solvents, and the results are summarized in Table 1. The spectra of **1**–**3** in cyclohexane are shown in Figure 1. The spectra of (*E*)-**1** and (*Z*)-**1** and those of (*E*)-**2** and (*Z*)-**2** were similar in shape, which indicated that the configuration of the $CF_3CH{=}CH$ moieties had little effect on the electronic structures of **1** and **2**. The absorption edges of **1** and **2** ranged from 348 to 360 nm, whereas that of **3** was at 406 nm. In addition, the effective conjugation length of (*E*)-**3** was the longest among **1**–**3**. In all compounds, a very small bathochromic shift was observed with respect to solvent polarity.[18] The absorption spectra of (*E*)-**3** in various solvents are illustrated in Figure 2 as a representative example.

The fluorescence properties of **1**–**3** in various solvents are summarized in Table 2. In cyclohexane, **1** and **2** exhibited violet luminescence with emission maxima (362–373 nm) in the UV region, whereas (*E*)-**3** yielded violet fluorescence with an emission maximum at 407 nm (Figure 3). In all compounds, the spectra redshifted as the solvent polarity increased, as exemplified by those of (*E*)-**3** in Figure 4. This phenomenon suggests that the excited states consist of charge-localized electronic structures. The fluorescence quantum yields (Φ_f) of **1**–**3** in solution ranged from low to moderate, with the highest value being for (*E*)-**2**. Investigation on the geometry of the trifluoropropenyl moiety in **1** and **2** revealed that *E* isomers ((*E*)-**1** and (*E*)-**2**) exhibited higher Φ_f values than *Z* isomers ((*Z*)-**1** and (*Z*)-**2**).

Table 1. UV/Vis absorption data of **1**–**3**.[a]

Solvent (ε)[b]	Absorption maximum [nm] (molar absorption coefficient [$M^{-1}cm^{-1}$])				
	(*E*)-**1**	(*Z*)-**1**	(*E*)-**2**	(*Z*)-**2**	(*E*)-**3**
c-C_6H_{12} (2.0)	304	301	324	312	360
	(10500)	(9000)	(5800)	(5600)	(9900)
Et_2O (4.3)	302	305	324	312	363
	(11600)	(8000)	(6300)	(6300)	(9700)
CH_2Cl_2 (9.1)	303	307	325	311	364
	(11000)	(7900)	(6300)	(7100)	(9000)
CH_3CN (37)	302	305	325	314	364
	(13400)	(8200)	(6400)	(6700)	(9400)
DMSO (47)	308	311	328	316	371
	(13400)	(10400)	(6400)	(7200)	(8700)

[a] Measured at 1×10^{-5} mol L. [b] ε: dielectric constants.

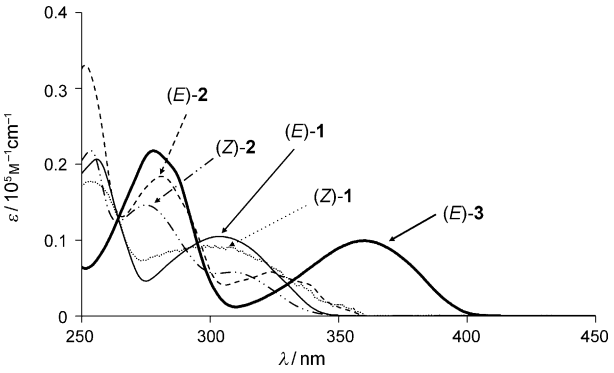

Figure 1. Absorption spectra of **1**–**3** in cyclohexane.

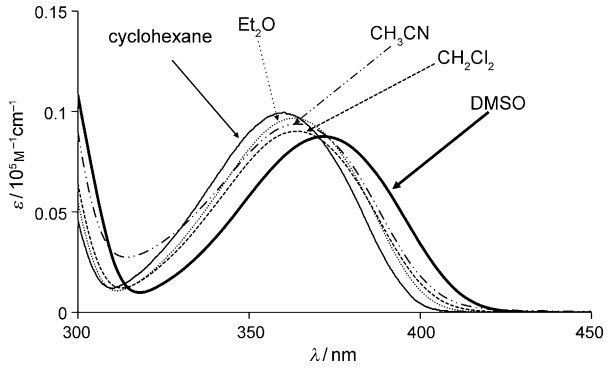

Figure 2. Absorption spectra of (*E*)-**3** in various solvents.

Table 2. Fluorescence data of **1**–**3**.[a]

Solvent[b]/film	Emission maximum [nm] (Φ_f)[c]				
	(*E*)-**1**	(*Z*)-**1**	(*E*)-**2**	(*Z*)-**2**	(*E*)-**3**
c-C_6H_{12}	362 (0.22)	373 (0.10)	366 (0.44)	364 (0.15)	407 (0.34)
Et_2O	370 (0.24)	370 (0.12)	370 (0.40)	370 (0.09)	420 (0.33)
CH_2Cl_2	379 (0.22)	378 (0.12)	374 (0.37)	370 (0.05)	425 (0.27)
CH_3CN	389 (0.15)	389 (0.11)	379 (0.23)	379 (0.04)	431 (0.18)
DMSO	392 (0.21)	400 (0.03)	383 (0.33)	379 (0.04)	438 (0.28)
neat thin film	406 (0.09)	409 (0.14)	400 (0.13)	392 (0.06)	434 (0.37)
PMMA film	379 (0.12)	384 (0.18)	409 (0.25)	413 (0.19)	428 (0.49)

[a] Excitation was effected by UV light at 265 nm. [b] Measured at 1×10^{-5} M. [c] Absolute quantum yield determined by a calibrated integrating sphere system. DMSO = dimethyl sulfoxide.

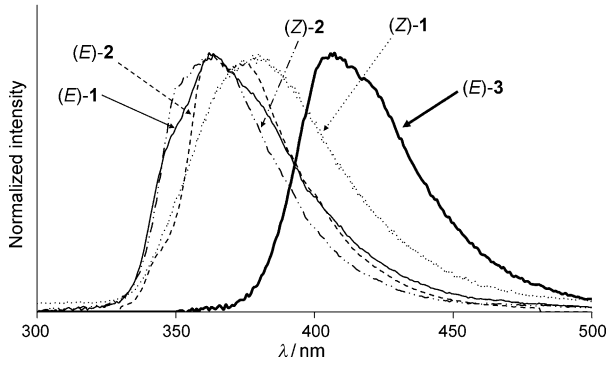

Figure 3. Fluorescence spectra of **1**–**3** in cyclohexane.

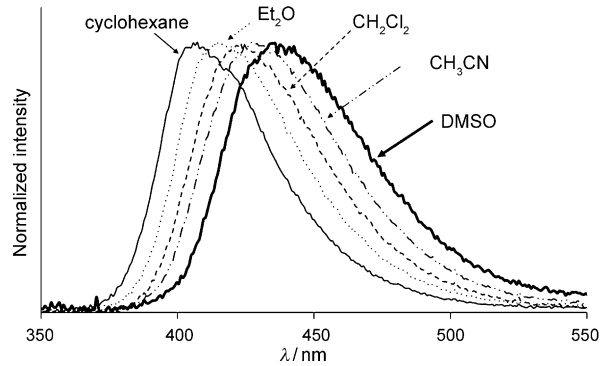

Figure 4. Fluorescence spectra of (*E*)-**3** in various solvents.

Since we observed that **1**–**3** exhibited luminescence upon UV irradiation on TLC, the fluorescence spectra of **1**–**3** in neat thin films and dispersed in poly(methyl methacrylate) (PMMA) films were measured. The neat thin films and doped PMMA films were prepared on quartz plates by spin-coating from dichloromethane solutions and chlorobenzene solutions dissolving PMMA (15 wt%), respectively. The results are summarized in Table 2 and the spectra are shown in Figures 5 and 6.[19] The emission maxima in the solid states appeared in the violet to blue region and exhibited a bathochromic shift when compared with those in solution. Quantum yields of **1** and **2** in the solid states ranged from 0.06 to 0.25, whereas (*E*)-**3** in both the neat thin film and the doped PMMA film produced good quantum yields (Φ_f = 0.37 and 0.49, respectively).

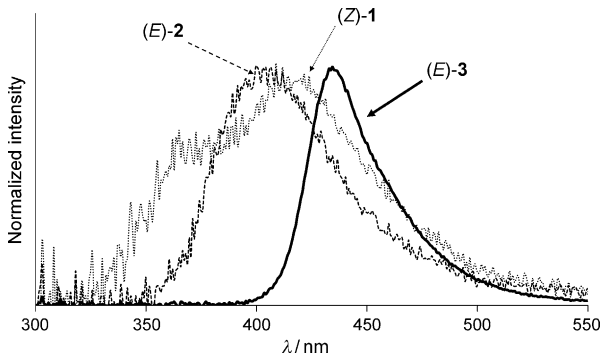

Figure 5. Fluorescence spectra of (*Z*)-**1**, (*E*)-**2**, and (*E*)-**3** in neat thin film.

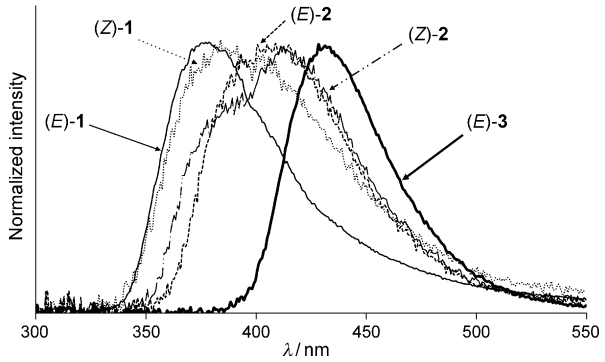

Figure 6. Fluorescence spectra of **1**–**3** dispersed in PMMA film.

To gain insight into the efficient luminescence of (*E*)-**3** in the solid state, we analyzed its single crystal obtained by recrystallization from a solvent mixture of dichloromethane and *n*-hexane by X-ray diffraction.[20] The molecules crystallize in a triclinic lattice with a space group $P\bar{1}$. The asymmetric unit is composed of two crystallographically independent molecules, both of which adopt a nearly identical conformation and have a center of symmetry at the centroid of the benzene ring. As shown in Figure 7, the main framework consisting of $CF_3CH{=}CH{-}$benzene$-CH{=}CHCF_3$ is slightly twisted, with dihedral angles between the central benzene plane and the $CF_3CH{=}CH$ moiety of 9 and 12°, respectively. A trifluoromethyl group adopts a bisected conformation with respect to an ethenyl plane, with a C–F(1) bond located in the benzene plane that bisects the bond angle of F(2)-C-F(3).

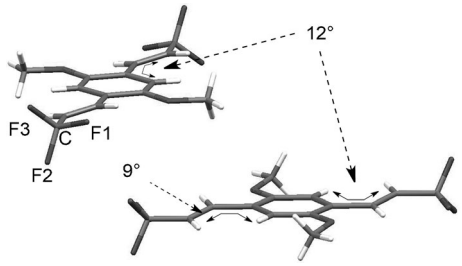

Figure 7. Molecular structure of (*E*)-**3** in a single crystal.

The packing diagram of (*E*)-**3** is shown in Figure 8. Each molecule forms a layer structure (Figure 8a) in which benzene rings in adjacent molecules are far apart from one another. While the distance between the benzene ring of a molecule in one layer and the ethenyl moiety of the closest molecule in the next layer is 3.7–3.8 Å, which may result in intermolecular electronic interactions, the angle formed by the long axes of the molecules is about 80° (Figure 8b). Theoretical calculations have suggested that cross-stacking should be advantageous to efficient solid-state luminescence;[21] therefore, the high quantum yield of (*E*)-**3** observed in the neat thin film can likely be attributed to the cross-stacked packing motif.

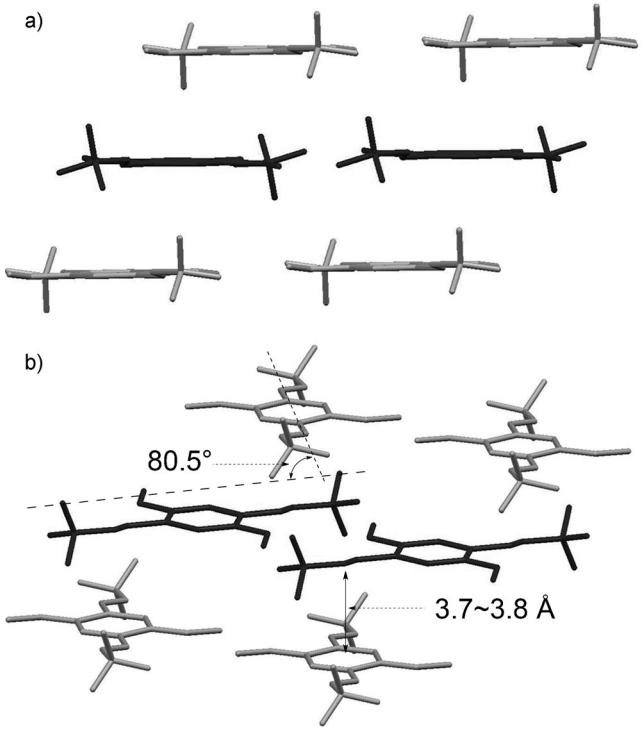

Figure 8. Crystal packing diagram of (*E*)-**3**: a) view from *b* axis, b) view from *a* axis. Each molecule is colored gray and black according to the symmetry equivalence in the crystal. Hydrogen atoms are omitted for clarity.

Theoretical Calculations

Theoretical calculations of (*E*)-**2** and (*E*)-**3**, which exhibited higher fluorescence quantum yields among **1**–**3**, were conducted by using the Gaussian 03 package with DFT to elucidate the electronic structures.[22] First, the ground-state geometries of (*E*)-**2** were optimized at the B3LYP/6-31G(d) level by using the six conformers (**A**–**F**) shown in Figure 9 as the initial structures. These structures gave rise to three conformers **G**–**I**, as local minima (Figure 10).[23] The methyl groups in all of the optimized structures were oriented to the opposite side with respect to the adjacent $CF_3CH{=}CH-$ moieties and positioned on the benzene plane. The structural differences among **G**–**I** were due to the orientation of (*E*)-$CF_3CH{=}CH-$ moieties against methoxy groups at their

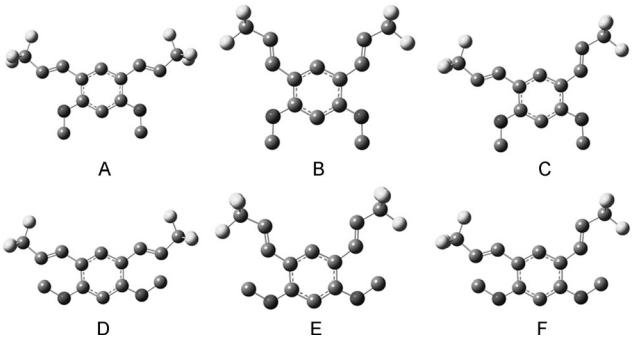

Figure 9. Conformers **A**–**F** of (*E*)-**2** as initial geometries for structural optimization. Hydrogen atoms are omitted for clarity.

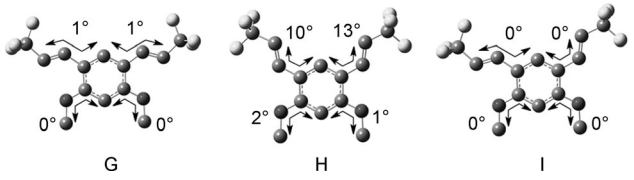

Figure 10. The optimized geometries **G**–**I** of (*E*)-**2** with the dihedral angles between the substituents and the benzene plane. Hydrogen atoms are omitted for clarity.

ortho-positions. Each (*E*)-$CF_3CH{=}CH-$ moiety of **G** and **I** was located on the same plane of the central benzene ring, whereas two (*E*)-$CF_3CH{=}CH-$ moieties of **H** deviated from a benzene plane by 10 and 13°, respectively. The most stable conformer was **G**; however, the energy differences among the three local minima were very small (0.19 kcal mol^{-1} for **H** and 0.097 kcal mol^{-1} for **I** with respect to **G**).

Structural optimization of (*E*)-**3** was conducted by using DFT at the B3LYP/6-31G(d) level with the structure obtained by X-ray crystallographic analysis as an initial coordinate. The optimized structure was almost identical to the initial structure (Figure 11). To gain insight into the effect of fluorine on the electronic structures of (*E*)-**2** and (*E*)-**3**, we also optimized their nonfluorinated analogues (*E*)-**2(H)** and (*E*)-**3(H)** by using the initial geometries defined by replac-

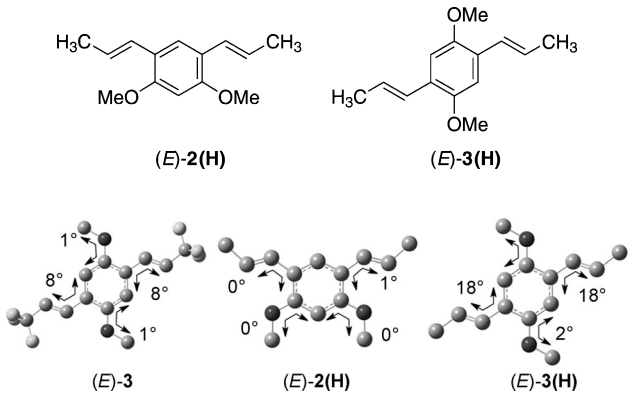

Figure 11. The optimized geometries of (*E*)-**3**, (*E*)-**2(H)**, and (*E*)-**3(H)** with the dihedral angles between the substituents and the benzene plane. Hydrogen atoms are omitted for clarity.

ing CF_3 in the initial geometries of (*E*)-**2** and (*E*)-**3** with CH_3. As shown in Figure 11, the calculated structures of **G** and (*E*)-**2(H)** did not differ, whereas the dihedral angles between the $CF_3CH{=}CH-$ moieties and the central benzene ring in (*E*)-**3(H)** were found to be larger than those in (*E*)-**3** (18° for (*E*)-**3(H)** and 8° for (*E*)-**3**). Thus, the presence of fluorine atoms in benzene derivatives of type **3** causes the conjugation between the two propenyl moieties and central benzene to be more efficient than in the fluorine-free counterpart.

HOMO and LUMO diagrams of (*E*)-**2** and (*E*)-**2(H)** with energy levels and gaps are shown in Figure 12. The HOMO and LUMO of (*E*)-**2** are slightly more extended over C-

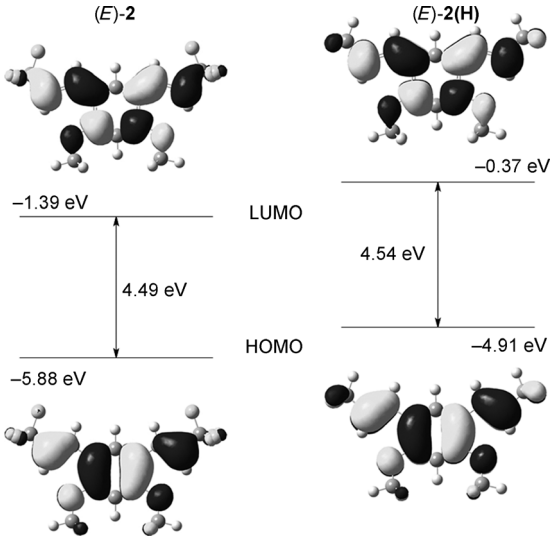

Figure 12. Energy level and orbital diagrams of the HOMOs and LUMOs of (*E*)-**2** and (*E*)-**2(H)**.

(sp^2)–CF_3 bonds than those of (*E*)-**2(H)**. The energy levels of both the HOMO and LUMO of (*E*)-**2** are lower than those of (*E*)-**2(H)**. Hence, the reduction in the energy levels of HOMO is ascribed to the conjugation between σ* orbitals of C–F bonds and the π orbitals of ethenyl moieties, whereas the decrease in the LUMO energy results from mixing of the σ* orbitals and the π* orbitals. Since the HOMO–LUMO gap of (*E*)-**2** is smaller than that of (*E*)-**2(H)**, the σ*–π* conjugation is more efficient than the σ–π* conjugation.

The same fluorine effect leading to slight extension of the frontier molecular orbitals and narrowing of the HOMO–LUMO gap was confirmed for (*E*)-**3** and (*E*)-**3(H)** (Figure 13). It is important to note that the two ethereal oxygen atoms participate in the HOMOs, but not in the LUMOs. Thus, the HOMO–LUMO transition of (*E*)-**3** includes charge transfer from the oxygen atoms to the $C(sp^2)$–CF_3 moieties. The time-dependent DFT calculation indicated that the absorption band around 360 nm corresponds to the HOMO–LUMO transition. These results are consistent

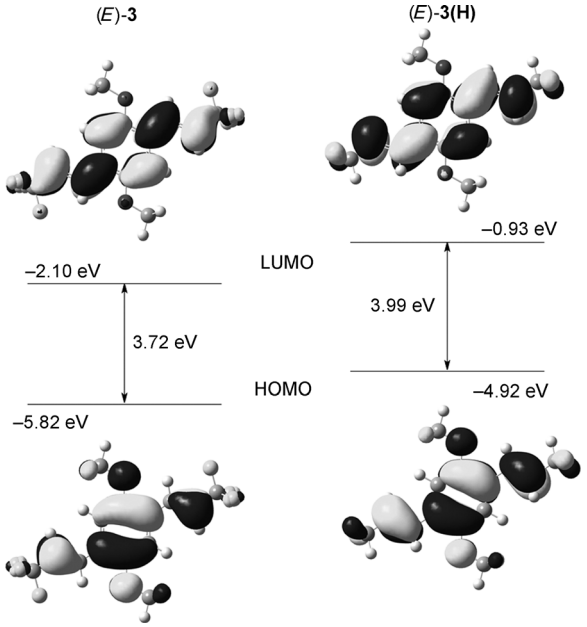

Figure 13. Energy level and orbital diagrams of the HOMOs and LUMOs of (*E*)-**3** and (*E*)-**3(H)**.

with bathochromic shift of the fluorescence spectra of (*E*)-**3** that was observed in various solvents.

Conclusions

We prepared and characterized five dimethoxybis(3,3,3-trifluoropropenyl)benzenes. All the benzene derivatives exhibited fluorescence in the violet region with low to good quantum yields in both the solution and the solid state. It should be noted that 1,4-dimethoxy-2,5-bis[(*E*)-3,3,3-trifluoropropenyl]benzene emits brilliant violet light in neat thin film and in doped PMMA film with emission maxima at 434 (Φ_f = 0.37) and 428 nm (Φ_f = 0.49), respectively. The fluorine atoms of the benzene derivatives contribute to extension of the frontier orbitals and a decrease in the energy gaps, allowing visible light luminescence from the compact π-conjugated system. This study shed light on the trifluoropropenyl moiety as a new entry of fluorinated π-modules that induce unique properties in functional organic materials.

Experimental Section

*Typical Procedure for the Palladium-Catalyzed Cross-Coupling Reaction of 3,3,3-Trifluoropropynylzinc Chloride with Diiodobenzene: Preparation of 1,2-Dimethoxy-4,5-bis(3,3,3-trifluoropropynyl)benzene (**7**)*

BuLi (1.4 mL, 2.2 mmol, 1.6 M in *n*-hexane) was added to a THF (5.1 mL) solution of 1,1-dichloro-3,3,3-trifluoro-2-tosyloxypropene (**4**, 0.34 g, 1.0 mmol) at −78 °C. The solution was stirred at −78 °C for 30 min before the addition of $ZnCl_2$·TMEDA (TMEDA = *N*,*N*,*N*',*N*'-tetramethyl-1,2-ethane, 0.28 g, 1.1 mmol) in one portion. The resulting solution was stirred at −78 °C for 30 min and at room temperature for an additional 30 min. The mixture was added to a THF (3.0 mL) solution of 1,2-diiodo-

4,5-dimethoxybenzene (**6**, 0.10 g, 0.26 mmol), $[PdCl_2(dppf)]\cdot CH_2Cl_2$ (21 mg, 26 μmol), and Ag_2O (59 mg, 0.26 mmol), and the resulting mixture was then heated at 80 °C for 15 h. Silica gel (1.0 g) and AcOEt (30 mL) were added to the reaction mixture and the slurry was concentrated in vacuo. Column chromatography on silica gel with the silica gel absorbed with the crude product (*n*-hexane/AcOEt 5:1) gave **7** (59 mg, 72 %) as a colorless solid. M.p. 99.0–99.6 °C; T_d (5 wt.%): 122.9 °C; R_f = 0.42 (*n*-hexane/AcOEt 4:1); ^{1}H NMR (400 MHz, $CDCl_3$): δ = 3.93 (s, 6H), 7.02 ppm (s, 2H); ^{13}C NMR (100 MHz, $CDCl_3$): δ = 56.2, 79.0 (q, J = 52.9 Hz), 83.6 (q, J = 6.9 Hz), 114.5, 114.7 (q, J = 256.8 Hz), 115.5, 151.0 ppm; ^{19}F NMR (282 MHz, $CDCl_3$): δ = −50.6 ppm; IR (KBr): $\tilde{\nu}$ = 2247, 1518, 1400, 1283, 1254, 1132, 999, 868, 718, 569 cm^{-1}; MS (EI): *m*/*z* (%): 322 (100) [M^+], 300 (20); elemental analysis calcd (%) for $C_{14}H_8F_6O_2$: C 52.19, H 2.50; found: C 52.00, H 2.75.

*Typical Procedure for the trans-Reduction of Alkynes with $LiAlH_4$: Preparation of 1,2-Dimethoxy-4,5-bis[(E)-3,3,3-trifluoropropenyl]benzene ((E)-**1**)*

$LiAlH_4$ (8.7 mg, 0.23 mmol) was added to a solution of **7** (29 mg, 91 μmol) in THF (0.28 mL) at room temperature. The resulting solution was stirred at room temperature for 1 h. The reaction mixture was quenched with sat. aq. NH_4Cl (10 mL) and extracted with AcOEt (10 mL × 3). The combined organic layer was dried over anhydrous $MgSO_4$ and concentrated in vacuo. The crude product was purified by column chromatography on silica gel (*n*-hexane/AcOEt 8:1) to give (*E*)-**1** (13 mg, 46 %) as a colorless solid. M.p. 124.2–125.2 °C; T_d (5 wt.%): 119.4 °C; R_f = 0.47 (*n*-hexane/AcOEt 4:1); ^{1}H NMR (400 MHz, $CDCl_3$): δ = 3.95 (s, 6H), 6.05 (dq, J = 16.0, 6.6 Hz, 2H), 6.94 (s, 2H), 7.39 ppm (dq, J = 16.0, 2.1 Hz, 2H); ^{13}C NMR (100 MHz, $CDCl_3$): δ = 56.2, 109.0, 117.6 (q, J = 33.6 Hz), 123.1 (q, J = 267.9 Hz), 125.8, 133.7 (q, J = 6.9 Hz), 150.3 ppm; ^{19}F NMR (282 MHz, $CDCl_3$): δ = −63.8 ppm (d, J = 6.6 Hz); IR (KBr): $\tilde{\nu}$ = 1601, 1516, 1319, 1283, 1097, 966, 665, 544 cm^{-1}; MS (EI): *m*/*z* (%): 326 (45) [M^+], 307 (12), 257 (100); elemental analysis calcd (%) for $C_{14}H_{12}F_6O_2$: C 51.54, H 3.71; found: C 51.63, H 4.00.

*Typical Procedure for the cis-Reduction of Alkynes: Preparation of 1,2-Dimethoxy-4,5-bis[(Z)-3,3,3-trifluoropropenyl]benzene ((Z)-**1**)*

A drop of quinoline and $Pd/BaSO_4$ (4.0 mg, 5 wt.%) were added to methanol (2.5 mL) at room temperature and the mixture was stirred for 10 min before the addition of **7** (80 mg, 0.25 mmol). The reaction mixture was stirred for another 10 min at room temperature and then filled with H_2 gas (1 atm.). The resulting solution was stirred at room temperature for 1 h and filtered through a pad of Celite and Florisil. The filtrate was concentrated in vacuo. The crude product was purified by GPC to give (*Z*)-**1** (75 mg, 93 %) as a colorless solid. M.p. 57.4–58.1 °C; T_d (5 wt.%): 109.7 °C; R_f = 0.45 *n*-hexane/AcOEt 4:1); ^{1}H NMR (400 MHz, $CDCl_3$): δ = 3.89 (s, 6H), 5.82 (dq, J = 12.4, 12.7 Hz, 2H), 6.90 (s, 2H), 6.92 ppm (d, J = 12.4 Hz, 2H); ^{13}C NMR (100 MHz, $CDCl_3$): δ = 56.2, 113.4, 119.1 (q, J = 33.9 Hz), 122.4 (q, J = 270.0 Hz), 125.4, 137.2 (q, J = 5.7 Hz), 148.7 ppm; ^{19}F NMR (282 MHz, $CDCl_3$): δ = −58.2 ppm (d, J = 12.7 Hz); IR (KBr): $\tilde{\nu}$ = 3011, 1717, 1508, 1279, 1134, 718, 419 cm^{-1}; MS (EI): *m*/*z* (%): 326 (78) [M^+], 307 (19), 257 (100), 242 (14), 188 (12); elemental analysis calcd (%) for $C_{14}H_{12}F_6O_2$: C 51.54, H 3.71; found: C 51.40, H 3.80.

*1,5-Dimethoxy-2,4-bis(3,3,3-trifluoropropynyl)benzene (**9**)*

Purified by column chromatography on silica gel (*n*-hexane/AcOEt 4:1); yield: 69 %; colorless solid; m.p. 169.5–170.2 °C; T_d (5 wt.%): 130.0 °C; R_f = 0.17 (*n*-hexane/AcOEt 4:1); ^{1}H NMR (400 MHz, $CDCl_3$): δ = 3.96 (s, 6H), 6.41 (s, 1H), 7.63 ppm (s, 1H); ^{13}C NMR (100 MHz, $CDCl_3$): δ = 56.2, 79.0 (q, J = 52.1 Hz), 82.1 (q, J = 6.4 Hz), 94.6, 100.6, 114.8 (q, J = 255.9 Hz), 139.6, 164.4 ppm; ^{19}F NMR (282 MHz, $CDCl_3$): δ = −49.9 ppm; IR (KBr): $\tilde{\nu}$ = 2247, 1609, 1506, 1290, 1175, 1111, 1020, 824, 552 cm^{-1}; MS (EI): *m*/*z* (%): 322 (100) [M^+], 303 (15), 253 (11); elemental analysis calcd (%) for $C_{14}H_8F_6O_2$: C 52.19, H 2.50; found: C 52.06, H 2.60.

*1,5-Dimethoxy-2,4-bis[(E)-3,3,3-trifluoropropenyl]benzene ((E)-**2**)*

Purified by column chromatography on silica gel (*n*-hexane/AcOEt 9:1); yield: 38 %; a colorless solid; m.p. 108.8–109.9 °C; T_d (5 wt.%): 130.8 °C; R_f = 0.36 (*n*-hexane/AcOEt 4:1); ^{1}H NMR (400 MHz, $CDCl_3$): δ = 3.94 (s, 6H), 6.26 (dq, J = 15.6, 5.4 Hz, 2H), 7.30 (dq, J = 15.6, 2.2 Hz, 2H), 7.46 ppm (s, 2H); ^{13}C NMR (100 MHz, $CDCl_3$): δ = 55.7, 94.8, 114.9 (q, J = 33.5 Hz), 115.1, 123.9 (q, J = 268.3 Hz), 129.1, 131.9 (q, J = 7.2 Hz), 160.2 ppm; ^{19}F NMR (282 MHz, $CDCl_3$): δ = −63.4 ppm (d, J = 5.4 Hz); IR (KBr): $\tilde{\nu}$ = 2949, 1651, 1614, 1471, 1304, 1269, 1117, 1028, 827, 519 cm^{-1}; MS (EI): *m*/*z* (%): 326 (100) [M^+], 307 (10); elemental analysis calcd (%) for $C_{14}H_{12}F_6O_2$: C 51.54, H 3.71; found: C 51.80, H 3.68.

*1,5-Dimethoxy-2,4-bis[(Z)-3,3,3-trifluoropropenyl]benzene ((Z)-**2**)*

Purified by GPC ($CHCl_3$); yield: 60 %; colorless solid; m.p. 89.7–91.2 °C; T_d (5 wt.%): 127.0 °C; R_f = 0.34 (*n*-hexane/AcOEt 4:1); ^{1}H NMR (400 MHz, $CDCl_3$): δ = 3.89 (s, 6H), 5.64–5.76 (m, 2H), 6.41 (s, 1H), 7.00 (d, J = 12.8 Hz, 2H), 7.47 ppm (s, 1H); ^{13}C NMR (100 MHz, $CDCl_3$): δ = 55.7, 93.7, 115.0, 116.8 (q, J = 34.8 Hz), 122.9 (q, J = 269.9 Hz), 131.1–131.3 (m), 133.9–134.0 (m), 159.1 ppm; ^{19}F NMR (282 MHz, $CDCl_3$): δ = −58.8 ppm (d, J = 7.6 Hz); IR (KBr): $\tilde{\nu}$ = 2982, 1612, 1497, 1319, 1209, 1115, 1026, 924, 822, 745, 559 cm^{-1}; MS (EI): *m*/*z* (%): 326 (100) [M^+], 307 (12); elemental analysis calcd (%) for $C_{14}H_{12}F_6O_2$: C 51.54, H 3.71; found: C 51.66, H 3.75.

*1,4-Dimethoxy-2,5-bis(3,3,3-trifluoropropynyl)benzene (**11**)*

Isolated in 84 % yield as a colorless solid; m.p. 116.8–117.6 °C; T_d (5 wt.%): 129.6 °C; R_f = 0.69 (*n*-hexane/AcOEt 4:1); ^{1}H NMR (400 MHz, $CDCl_3$): δ = 3.87 (s, 6H), 7.02 ppm (s, 2H); ^{13}C NMR (100 MHz, $CDCl_3$): δ = 56.5, 81.2 (q, J = 52.9 Hz), 82.2 (q, J = 6.1 Hz), 111.3, 114.7 (q, J = 257.1 Hz), 116.2, 154.9 ppm; ^{19}F NMR (282 MHz, $CDCl_3$): δ = −50.5 ppm. IR (KBr): $\tilde{\nu}$ = 2259, 1506, 1402, 1288, 1134, 1030, 868, 667 cm^{-1}; MS (EI): *m*/*z* (%): 322 (100) [M^+], 307 (45); elemental analysis calcd (%) for $C_{14}H_8F_6O_2$: C 52.19, H 2.50; found: C 51.90, H 2.56.

*1,4-Dimethoxy-2,5-bis[(E)-3,3,3-trifluoropropenyl]benzene ((E)-**3**)*

$Pd/BaCO_3$ (5.0 mg, 5 wt.%) was added to pyridine (3.5 mL) in a Schlenk tube at room temperature, and then the mixture was stirred for 10 min before the addition of **11** (0.10 g, 0.31 mmol). After another 10 min of stirring, the tube was filled with H_2 gas and the whole mixture was stirred at room temperature for 2 h. The resulting solution was filtered with a pad of Celite and Florisi and the filtrate was concentrated in vacuo. The crude product was purified by column chromatography on silica gel (*n*-hexane/AcOEt 4:1), giving a mixture of (*Z*)-**3** and (*E*)-**3** (*Z*/*E* 2:1, 99 mg, 97 %) as a colorless solid. I_2 (2.0 mg, 7.9 μmol) was added to a $CHCl_3$ (10 mL) solution of the mixture (29 mg, 89 μmol). The mixture was stirred under irradiation of UV light (UVA-100HA Riko) at room temperature for 8 h before quenching with sat. aq. $Na_2S_2O_3$ (10 mL). The aqueous layer was extracted with AcOEt (10 mL × 3). The combined organic layer was dried over anhydrous $MgSO_4$ and concentrated in vacuo. The residue was purified by column chromatography on silica gel (*n*-hexane/AcOEt 6:1) to give only (*E*)-**3** (22 mg, 77 %) as a colorless solid. M.p. 159.5–160.2 °C; T_d (5 wt.%): 147.4 °C; R_f = 0.63 (*n*-hexane/AcOEt 4:1); ^{1}H NMR (400 MHz, $CDCl_3$): δ = 3.88 (s, 6H), 6.36 (dq, J = 16.4, 7.9 Hz, 2H), 6.94 (s, 2H), 7.39 (dq, J = 16.4, 2.4 Hz, 2H), 7.47 ppm (s, 1H); ^{13}C NMR (100 MHz, $CDCl_3$): δ = 56.1, 111.0, 117.5 (q, J = 33.5 Hz), 123.6 (q, J = 268.4 Hz), 124.3, 132.3 (q, J = 6.7 Hz), 151.9 ppm; ^{19}F NMR (282 MHz, $CDCl_3$): δ = −63.7 ppm (d, J = 7.9 Hz); IR (KBr): $\tilde{\nu}$ = 3017, 1661, 1499, 1414, 1310, 1281, 1215, 1111, 1040, 970, 905, 654 cm^{-1}; MS (EI): *m*/*z* (%): 326 (100) [M^+], 311 (11), 242 (10); elemental analysis calcd (%) for $C_{14}H_{12}F_6O_2$: C 51.54, H 3.71; found: C 50.99, H 3.99.

*UV/Vis and Fluorescence Spectra of **1**–**3** in Solvents*

Spectroscopic-grade solvents for measurements of UV/Vis absorption and fluorescence spectra were purchased from Kanto Chemical Co. and degassed by bubbling with argon before use. UV/Vis and fluorescence spectra of **1**–**3** in solvents were measured with 1×10^{-5} M solution prepared from degassed spectroscopic-grade cyclohexane. UV/Vis absorption spectra were measured with a Shimadzu UV-2550 spectrometer.

Fluorescence spectra were measured by Hamamatsu Photonics C9920–02 Absolute PL Quantum Yield Measurement System and absolute quantum yields were determined by using a calibrated integrating sphere system. The absolute quantum yields were obtained by averaging values of three to five measurements with different lots of samples.

*Typical Procedure for the Preparation of Spin-Coated Films of **1–3***

In a glass tube, (*E*)-**2** (2.0 mg) was dissolved in CH_2Cl_2 (0.50 mL). The resulting solution was dropped onto a quartz plate (10 mm × 10 mm) and spin-coated with a MIKASA MS-A-100 spin coater at 100 rpm over a period of 300 s. The deposited film was dried under reduced pressure at room temperature for 2 h.

*Typical Procedure for the Preparation of PMMA Films Doped with **1–3***

In a glass tube, (*E*)-**3** (5.0 mg) was dissolved in a PMMA chlorobenzene solution (15 wt.%, 1.00 mL). The resulting solution was dropped onto a quartz plate (10 × 10 mm) and spin-coated with a MIKASA MS-A-100 spin coater at 300 rpm for 20 s and then at 100 rpm over a period of 280 s. The film was dried under reduced pressure at room temperature for 1.5 h.

Molecular Orbital Calculations

Molecular structures were optimized by DFT methods at the B3LYP/6-31G(d) level by using the Gaussian 03 package. Cartesian coordinates for the geometry optimization study are listed in the Supporting Information. Energy levels of molecular orbitals were calculated at the B3LYP/6-31G(d) level.

Acknowledgements

This work was supported by Grants-in-Aid for Creative Scientific Research, no. 16GS0209 and Scientific Research, no. 22350081, from the Ministry of Education, Culture, Sports, Science and Technology, Japan.

[1] a) M. Pagliaro, R. Ciriminna, *J. Mater. Chem.* **2005**, *15*, 4981–4991; b) F. Babudri, G. M. Farinola, F. Naso, R. Ragni, *Chem. Commun.* **2007**, 1003–1022.

[2] a) Y. Sakamoto, T. Suzuki, M. Kobayashi, Y. Gao, Y. Fukai, Y. Inoue, F. Sato, S. Tokito, *J. Am. Chem. Soc.* **2004**, *126*, 8138–8140; b) Y. Inoue, Y. Sakamoto, T. Suzuki, M. Kobayashi, Y. Gao, S. Tokito, *Jpn. J. Appl. Phys.* **2005**, *44*, 3663–3668.

[3] a) F. Babudri, A. Cardone, G. M. Farinola, F. Naso, *Tetrahedron* **1998**, *54*, 14609–14616; b) S. B. Heidenhain, Y. Sakamoto, T. Suzuki, A. Miura, H. Fujikawa, T. Mori, S. Tokito, Y. Taga, *J. Am. Chem. Soc.* **2000**, *122*, 10240–10241; c) S. Komatsu, Y. Sakamoto, T. Suzuki, S. Tokito, *J. Solid State Chem.* **2002**, *168*, 470–473.

[4] a) A. Facchetti, Y. Deng, A. Wang, Y. Koide, H. Sirringhaus, T. J. Marks, R. H. Friend, *Angew. Chem.* **2000**, *112*, 4721–4725; *Angew. Chem. Int. Ed.* **2000**, *39*, 4547–4551; b) A. Facchetti, M. Mushrush, M. H. Yoon, G. R. Hutchison, M. A. Ratner, T. J. Marks, *J. Am. Chem. Soc.* **2004**, *126*, 13859–13874.

[5] a) A. Facchetti, J. Letizia, M. H. Yoon, M. Mushrush, H. E. Katz, T. J. Marks, *Chem. Mater.* **2004**, *16*, 4715–4727; b) S. Ando, J. I. Nishida, H. Tada, Y. Inoue, S. Tokito, Y. Yamashita, *J. Am. Chem. Soc.* **2005**, *127*, 5336–5337.

[6] Y. Ie, Y. Umemoto, M. Nitani, Y. Aso, *Pure Appl. Chem.* **2008**, *80*, 589–597.

[7] a) R. Riehn, J. Morgado, R. Iqbal, S. C. Moratti, A. B. Holmes, S. Volta, F. Cacialli, *Macromolecules* **2000**, *33*, 3337–3341; b) F. Babudri, A. Cardone, L. Chiavarone, G. Ciccarella, G. M. Farinola, F. Naso, G. Scamarcio, *Chem. Commun.* **2001**, 1940–1941; c) F. Babudri, A. Cardone, G. M. Farinola, F. Naso, T. Cassano, L. Chiavarone, R. Tommasi, *Macromol. Chem. Phys.* **2003**, *204*, 1621–1627.

[8] M. Hird, *Chem. Soc. Rev.* **2007**, *36*, 2070–2095.

[9] a) *Highly Efficient OLEDs with Phosphorescent Materials* (Ed.: H. Yersin), Wiley-VCH, Weinheim, **2008**; b) *Organic Light-Emitting Devices. Synthesis Properties and Applications* (Eds.: K. Müllen, U. Scherf), Wiley-VCH, Weinheim, **2006**; c) R. H. Friend, R. W. Gymer, A. B. Holmes, J. H. Burroughes, R. N. Marks, C. Taliani, D. D. C. Bradley, D. A. Dos Santos, J. L. Brédas, M. Lögdlund, W. R. Salaneck, *Nature* **1999**, *397*, 121–128.

[10] a) J. Zaumseil, H. Sirringhaus, *Chem. Rev.* **2007**, *107*, 1296–1323; b) F. Cicoira, C. Santato, *Adv. Funct. Mater.* **2007**, *17*, 3421–3434.

[11] a) I. D. W. Samuel, G. A. Turnbull, *Chem. Rev.* **2007**, *107*, 1272–1295; b) I. D. W. Samuel, G. A. Turnbull, *Mater. Today* **2004**, *7*, 28–35; c) U. Scherf, S. Riechel, U. Lemmer, R. F. Mahrt, *Curr. Opin. Solid State Mater. Sci.* **2001**, *5*, 143–154; d) M. D. McGehee, A. J. Heeger, *Adv. Mater.* **2000**, *12*, 1655–1668; e) G. Kranzelbinder, G. Leising, *Rep. Prog. Phys.* **2000**, *63*, 729–762; f) N. Tessler, *Adv. Mater.* **1999**, *11*, 363–370; g) V. G. Kozlov, S. R. Forrest, *Curr. Opin. Solid State Mater. Sci.* **1999**, *4*, 203–208.

[12] For reviews on fluorescent sensors, see: a) S. W. Thomas Iii, G. D. Joly, T. M. Swager, *Chem. Rev.* **2007**, *107*, 1339–1386; b) L. Basabe-Desmonts, D. N. Reinhoudt, M. Crego-Calama, *Chem. Soc. Rev.* **2007**, *36*, 993–1017; c) O. S. Wolfbeis, *J. Mater. Chem.* **2005**, *15*, 2657–2669; d) J. F. Callan, A. P. de Silva, D. C. Magri, *Tetrahedron* **2005**, *61*, 8551–8588; e) R. Martinez-Manez, F. Sancenon, *Chem. Rev.* **2003**, *103*, 4419–4476; f) A. P. de Silva, H. Q. N. Gunaratne, T. Gunnlaugsson, A. J. M. Huxley, C. P. McCoy, J. T. Rademacher, T. E. Rice, *Chem. Rev.* **1997**, *97*, 1515–1566; selected examples of solid-state fluorescent sensors: g) S. Sreejith, K. P. Divya, A. Ajayaghosh, *Chem. Commun.* **2008**, 2903–2905; h) T. J. Dale, J. Rebek, *J. Am. Chem. Soc.* **2006**, *128*, 4500–4501; i) S. W. Zhang, T. M. Swager, *J. Am. Chem. Soc.* **2003**, *125*, 3420–3421; j) J. S. Yang, T. M. Swager, *J. Am. Chem. Soc.* **1998**, *120*, 11864–11873; k) J. S. Yang, T. M. Swager, *J. Am. Chem. Soc.* **1998**, *120*, 5321–5322.

[13] For a review on small organic molecules exhibiting highly efficient solid-state fluorescence, see: M. Shimizu, T. Hiyama, *Chem. Asian J.* **2010**, *5*, 1516–1531.

[14] M. Shimizu, Y. Takeda, M. Higashi, T. Hiyama, *Angew. Chem.* **2009**, *121*, 3707–3710; *Angew. Chem. Int. Ed.* **2009**, *48*, 3653–3656.

[15] a) M. Shimizu, M. Higashi, Y. Takeda, M. Murai, G. Jiang, Y. Asai, Y. Nakao, E. Shirakawa, T. Hiyama, *Future Med. Chem.* **2009**, *1*, 921–945; b) T. Konno, J. Chae, M. Kanda, G. Nagai, K. Tamura, T. Ishihara, H. Yamanaka, *Tetrahedron* **2003**, *59*, 7571–7580.

[16] When the coupling reaction was performed in the absence of Ag_2O or in the presence of a catalytic amount of Ag_2O (20 mol%), the yields of **7** were very low (10–21%). The use of $[Pd(PPh_3)_4]$ as a catalyst and one equivalent of Ag_2O also failed.

[17] A catalyst system of $[PdCl_2(dppf)]\cdot CH_2Cl_2$ (10 mol%) and Ag_2O (1.0 equiv) was less effective; the ^{19}F NMR spectroscopic yield of **9** was 51%.

[18] Dielectric constants (ε) in Table 1 were cited from B. Valeur, *Molecular Fluorescence*, Wiley-VCH: Weinheim, **2002**, p. 211.

[19] Because the signal-to-noise ratios of the spectra of (*E*)-**1** and (*Z*)-**2** in neat thin film were very low owing to the low quantum yields, the spectra were not shown in Figure 5 for clarity.

[20] CCDC 812204 ((*E*)-**3**) contains the supplementary crystallographic data for this paper. These data can be obtained free of charge from The Cambridge Crystallographic Data Centre via www.ccdc.cam.ac.uk/data_request/cif.

[21] a) J. Cornil, D. Beljonne, J. P. Calbert, J. L. Brédas, *Adv. Mater.* **2001**, *13*, 1053–1067; b) J. Cornil, *J. Am. Chem. Soc.* **1998**, *120*, 1289–1299; c) Z. Xie, B. Yang, F. Li, G. Cheng, L. Liu, G. Yang, H. Xu, L. Ye, M. Hanif, S. Liu, D. Ma, Y. Ma, *J. Am. Chem. Soc.* **2005**, *127*, 14152–14153.

[22] Gaussian 03, Revision E.01, M. J. Frisch, G. W. Trucks, H. B. Schlegel, G. E. Scuseria, M. A. Robb, J. R. Cheeseman, J. A. Montgomery, T. Vreven, K. N. Kudin, J. C. Burant, J. M. Millam, S. S. Iyengar, J. Tomasi, V. Barone, B. Mennucci, M. Cossi, G. Scalmani, N. Rega, G. A. Petersson, H. Nakatsuji, M. Hada, M. Ehara, K. Toyota, R. Fukuda, J. Hasegawa, M. Ishida, T. Nakajima, Y. Honda, O. Kitao, H. Nakai, M. Klene, X. Li, J. E. Knox, H. P. Hratchian, J. B. Cross,

V. Bakken, C. Adamo, J. Jaramillo, R. Gomperts, R. E. Stratmann, O. Yazyev, A. J. Austin, R. Cammi, C. Pomelli, J. W. Ochterski, P. Y. Ayala, K. Morokuma, G. A. Voth, P. Salvador, J. J. Dannenberg, V. G. Zakrzewski, S. Dapprich, A. D. Daniels, M. C. Strain, O. Farkas, D. K. Malick, A. D. Rabuck, K. Raghavachari, J. B. Foresman, J. V. Ortiz, Q. Cui, A. G. Baboul, S. Clifford, J. Cioslowski, B. B. Stefanov, G. Liu, A. Liashenko, P. Piskorz, I. Komaromi, R. L. Martin, D. J. Fox, T. Keith, A. Laham, C. Y. Peng, A. Nanayakkara, M. Challacombe, P. M. W. Gill, B. Johnson, W. Chen, M. W. Wong, C. Gonzalez, J. A. Pople, Gaussian, Inc., Wallingford CT, **2004**.

[23] Cartesian coordinates of the initial structures and the optimized structures are listed in the Supporting Information.

Received: February 22, 2011
Published online: June 30, 2011

